atmosphere

MDPI

Article

Mercury Pollution in Terrestrial Ecosystems of North Macedonia: Insights from an 18-Year Moss Biomonitoring Programme

Katerina Bačeva Andonovska [1], Robert Šajn [2,*], Jasminka Alijagić [2,*], Trajče Stafilov [1,3] and Lambe Barandovski [4]

[1] Research Centre for Environment and Materials, Academy of Sciences and Arts of the Republic of North Macedonia—MASA, Krste Misirkov 2, 1000 Skopje, North Macedonia
[2] Geological Survey of Slovenia, Dimičeva 14, 1000 Ljubljana, Slovenia
[3] Institute of Chemistry, Faculty of Natural Sciences and Mathematics, Ss. Cyril and Methodius University, P.O. Box 162, 1000 Skopje, North Macedonia
[4] Institute of Physics, Faculty of Natural Sciences and Mathematics, Ss. Cyril and Methodius University, P.O. Box 162, 1000 Skopje, Macedonia; lambe@pmf.ukim.mk
* Correspondence: robert.sajn@geo-zs.si (R.Š.); jasminka.alijagic@geo-zs.si (J.A.)

Abstract

Moss biomonitoring was conducted in 2002, 2005, 2010, 2015 and 2020 to evaluate atmospheric mercury (Hg) deposition across N. Macedonia as part of a comprehensive survey of potentially toxic elements (PTEs). More than 70 samples of the dominant moss species *Hypnum cupressiforme* and *Homalothecium lutescens* were collected during the summer field campaigns. Mercury concentrations were determined using cold vapour atomic absorption spectrometry and inductively coupled plasma mass spectrometry (ICP-MS). The results revealed marked temporal fluctuations: median Hg content increased from 56 μg/kg in 2002 to 68 μg/kg in 2005, peaked at 93 μg/kg in 2010, then decreased to 84 μg/kg in 2015, and further to 52 μg/kg in 2020. Over the study period, Hg concentrations ranged from 10 to 595 μg/kg, with the highest variability observed in 2010. Spatial distribution maps and regional comparisons indicate that elevated Hg contents correspond predominantly to anthropogenic sources, particularly in industrialised zones and regions affected by mining and metallurgical activities. The 2020 dataset shows a significantly lower median value (52 μg/kg) compared to previous surveys, indicating a slight improvement in air quality, although local hotspots persist. These results highlight the importance of long-term moss biomonitoring as a cost-effective approach for tracking atmospheric mercury trends and informing national environmental policy.

Keywords: atmospheric mercury; moss biomonitoring; potentially toxic elements; ICP-MS; North Macedonia

Received: 10 November 2025
Revised: 16 December 2025
Accepted: 19 December 2025
Published: 22 December 2025

1. Introduction

Air pollution encompasses a wide range of chemical elements and compounds released into the atmosphere, which can negatively impact ecosystems and human health [1]. Particulate matter is one of the most significant atmospheric pollutants, particularly PM2.5, which poses serious health risks due to its ability to penetrate deep into the respiratory system [1,2] and originates from diverse anthropogenic sources, including industrial processes, mining activities, and urbanisation. However, natural processes such as

volcanism, forest fires, oceanic emissions, and the decomposition of organic matter also contribute to atmospheric inputs. Particles can be released directly into the air as "primary PM," or they can form in the atmosphere as "secondary particles" from gaseous precursors such as ammonia, sulphur dioxide, and nitrogen oxides. Particulate matter (PM) is commonly classified by aerodynamic diameter, including PM10 (particles ≤ 10 μm), PM2.5 (particles ≤ 2.5 μm), and ultrafine particles (≤0.1 μm). PM2.5 refers to fine inhalable particles that can penetrate deep into the respiratory tract and pose significant health risks. Recent assessments from the EEA indicate that, in Europe, agriculture contributes significantly to PM2.5 formation through ammonia-driven secondary nitrate production, whereas residential heating remains the dominant source of PM2.5 emissions in many regions [3,4].

Mercury is one of the most critical pollutants because it is persistent, mobile, and has serious effects on human health. While Hg occurs naturally in the Earth's crust, it is released into the atmosphere mainly as elemental vapour. Natural emissions originate from volcanic eruptions, erosion of mineralised deposits, forest fires, and uncontrolled coal fires. The largest anthropogenic contributions are from fossil-fuel combustion, artisanal and small-scale gold mining (ASGM), non-ferrous metal production, cement manufacturing, and waste disposal. Recent global inventories [5–9] estimate natural mercury emissions at approximately 4000 Mg/yr, while anthropogenic emissions range from 2200 to 2600 Mg/yr, with ASGM identified as the single largest human source. These updated values reflect improved methodologies and more accurate reporting compared with earlier estimates. According to the EDGAR v8.1 global mercury emissions inventory, most of current anthropogenic mercury emissions originate from artisanal and small-scale gold mining, coal combustion, non-ferrous metal and cement production, waste incineration, and other industrial processes [10]. The Minamata Convention on Mercury, a global treaty adopted in 2013 and implemented through subsequent reports and assessments, provides the international policy framework for reducing mercury emissions and releases. Its objectives emphasise the importance of monitoring and controlling mercury sources, highlighting the relevance of long-term biomonitoring studies as a key tool for tracking environmental trends and supporting compliance with global mercury reduction efforts [11].

Elevated Hg contents in humans are associated with neurotoxicity, impaired hearing and vision, immunosuppression, cardiovascular risks, reproductive disorders, and irreversible damage to the nervous system [12]. Therefore, reliable monitoring of Hg emissions and depositions is of global importance.

The utilisation of mosses as biomonitors for atmospheric deposition was first proposed in the 1960s by Rühling and Tyler [13]. Mosses possess unique physiological characteristics, notably the absence of roots and the ability to absorb water and nutrients directly from the atmosphere, rendering them highly effective accumulators of airborne contaminants. This trait also enables mosses to accurately reflect deposition and pollutant concentrations in mining regions, with minimal interference from soil contamination [14,15].

Atmospheric heavy metal pollution can be effectively monitored using mosses due to their capacity to accumulate metals on their surfaces. Two principal approaches exist: the use of native moss species [16–19] and the moss-bag technique [20–24]. The use of native moss species avoids the logistical challenges associated with installing and maintaining deposition samplers over large areas. Since 1990, the European moss survey has been organised every five years [25–28], with the most recent 2020 campaign conducted in more than 35 countries [29]. The surveys provide valuable data on a range of PTEs (As, Cd, Cr, Cu, Fe, Hg, Ni, Pb, V, Zn) as well as nitrogen [29–32].

Harmens et al. (2010, 2015) [28,33] present key findings from the European moss surveys, which use mosses as effective biomonitors of atmospheric heavy metal and nitrogen

deposition. Their 2010 study reported significant decreases in heavy metal concentrations in mosses since 1990, reflecting improved air quality across Europe, although some industrial and mining regions remained hotspots. The follow-up in 2015 confirmed trends of declining heavy metal and nitrogen levels up to 2010 while highlighting persistent elevated levels in parts of eastern and southeastern Europe [28,33].

Moss biomonitoring also extends to mercury pollution, with Bargagli (2016) [34] emphasising the role of moss and lichens in tracking atmospheric mercury deposition. Furthermore, García-Seoane et al. (2023) [35] compared aquatic and terrestrial moss species, highlighting species-specific metal uptake mechanisms and confirming moss biomonitoring's adaptability across varied environments. Additionally, moss-bag techniques have been employed to capture atmospheric particulate matter, revealing that the quantity and composition of PM collected are closely linked to moss trace element uptake and the surrounding land-use types [36]. Fernández et al. (2015) [37] underscored the necessity of standardised protocols to ensure data comparability across studies and regions, noting that environmental conditions such as air humidity, wind intensity, and precipitation can influence heavy metal concentrations in mosses. In North Macedonia, the first nationwide survey of atmospheric mercury (Hg) deposition using mosses was conducted in 2002, followed by subsequent campaigns in 2005, 2010, 2015 and most recently in 2020 as part of a wider European monitoring programme [29,38–45]. Parallel investigations revealed elevated Hg accumulation in soils, especially near industrial centres such as the city of Veles, where emissions from a lead–zinc smelter have caused Hg soil contents to exceed more than three times the European average [46]. Further investigations in the Kavadarci region revealed both geogenic and anthropogenic contributions, with Hg levels reaching 3.8 mg/kg in some topsoil samples [47]. Elevated Hg levels were also detected near the Allchar deposit, a naturally mineralised As-Sb-Tl ore body south of Kavadarci, which, although of lithogenic origin, contributes to local air pollution [48]. This study aims to analyse the temporal trends of Hg content in moss samples collected during the surveys from 2002 to 2020 in N. Macedonia, identify the pollution hotspots, distinguish natural from anthropogenic influences, evaluate deposition patterns and compare the results from affected areas with those from background sites. The integration of moss biomonitoring data with soil studies provides comprehensive insight into mercury distribution and sources across the region.

2. Materials and Methods

2.1. Study Area

North Macedonia is a small landlocked country situated in the central part of the Balkan Peninsula, bordered by Serbia and Kosovo to the north, Bulgaria to the east, Albania to the west and Greece to the south (Figure 1). Covering an area of 25,713 km^2, it features complex geology and diverse landscapes, ranging from high mountain massifs (Šar Planina, Jakupica, and Osogovo) to fertile valleys such as the Vardar River Basin. The climate is transitional, combining Mediterranean and continental influences with hot, dry summers and relatively cold winters. The average annual precipitation varies considerably, ranging from less than 500 mm in the Vardar Valley to more than 1000 mm in the mountainous areas. The population of nearly two million is predominantly concentrated in urban centres, with Skopje as the capital and largest city. Industrial activity is unevenly distributed but plays a key role in regional pollution. The most significant sources of potentially toxic elements (PTEs) include the lead–zinc smelter in Veles, the ferronickel plant near Kavadarci, mining operations in Sasa and Toranica, and the "Allchar" deposit on Kožuf Mountain, known for its unique thallium, arsenic, and antimony mineralisation. Other polluters include thermal power plants, cement production, smaller industrial plants, and agriculture.

https://doi.org/10.3390/atmos17010012

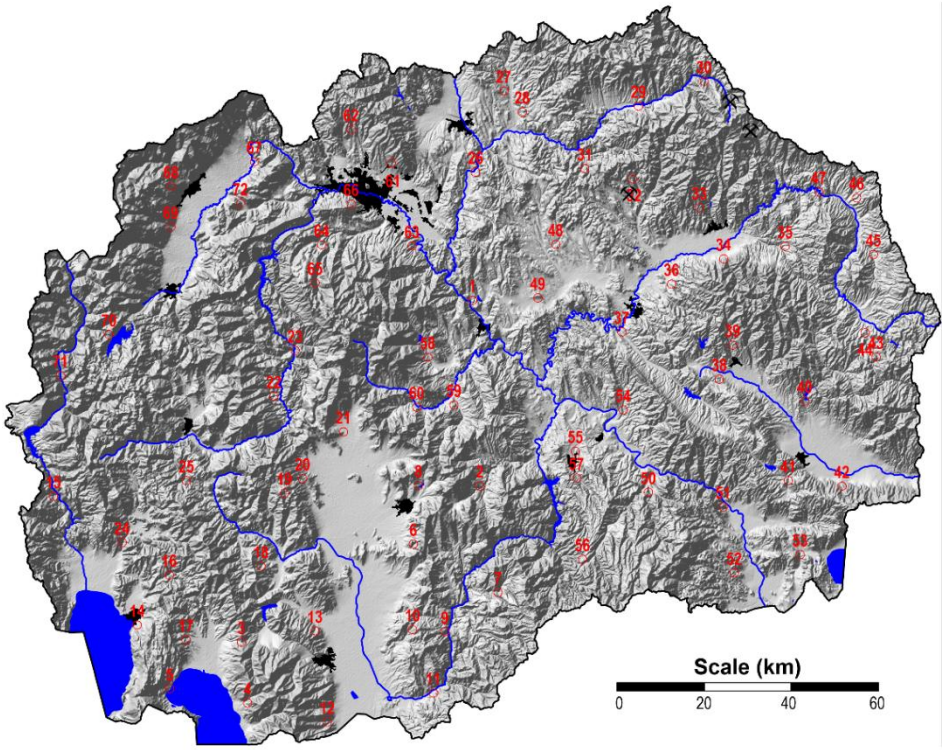

Figure 1. Shaded relief map of N. Macedonia with the sampling locations.

The geographical location, combined with the prevailing wind systems along the Vardar Valley, favours the regional transport of air pollutants, while topographical barriers can cause local accumulation. These natural and anthropogenic factors together determine the spatial distribution of atmospheric deposition in the country. Detailed descriptions of N. Macedonia's location, climate, demography, and industrial history are available in previous studies [49,50].

2.2. Sampling, Sample Preparation, and Instrumentation

Moss surveys were conducted in 2002, 2005, 2010, 2015 and 2020, covering the entire area of N. Macedonia [29,38–45]. A total of 72 samples were collected during each campaign (Figure 1). Sampling focused on the two most widespread carpet-forming species in the region, *Hypnum cupressiforme* and *Homalothecium lutescens*. At sites where both species were present, comparison revealed no statistically significant differences within analytical error, confirming their suitability as interchangeable biomonitors.

The sampling design and methodology followed the standardised protocol of the European moss survey [25,26,51–53], ensuring spatial comparability and long-term reliability of the data. Only young, green parts of the moss shoots were sampled to minimise variability due to plant age and external contamination. The samples were transported in clean paper bags, air-dried at room temperature and properly labelled and stored in paper bags.

The samples were digested in a microwave system. Approximately 0.5 g of collected material was placed in specialised Teflon vessels. In addition, 7 mL of concentrated nitric acid (HNO_3, 69%) and 2 mL of hydrogen peroxide (H_2O_2, 30%) were added, and the prepared mixture was left overnight. The programme used for digestion of moss samples involved heating at 180 °C for 20 min. The samples were then cooled to below 35 °C, filtered, and collected in 25 mL calibrated flasks. Mercury concentrations were analysed using cold vapour atomic absorption spectrometry (SpectrAA 55B; Varian, Palo Alto, CA, USA) using a continuous flow vapour generation accessory (VGA-76; Varian, Palo Alto,

CA, USA). Samples from the 2020 survey were analysed by inductively coupled plasma mass spectrometry (ICP-MS) applying the same digestion method as previously. The limit of detection (LOD) and limit of quantification (LOQ) for both techniques were 10 μg/kg and 3 μg/kg, respectively.

2.3. Quality Control

The quality control of Hg determination was based on the standard addition method, with recoveries ranging from 98.5% to 101.2%. Quality control was also ensured by analysing the standard moss reference materials M2 and M3, which are prepared for the European Moss Survey [51]. The results obtained are within the proposed ranges for the reference samples.

2.4. Statistical Methods and Mapping

Basic statistical parameters provide a numerical summary of a dataset's key characteristics. These parameters include measures such as the minimum and maximum values, mean (average), median (middle value), and mode (most frequent value), as well as measures of dispersion (or variability), such as variance and standard deviation, which describe how spread out the data is [54–56]. The statistical analysis of the data from the studies was conducted using Statistica 14 software [57].

Universal Kriging techniques were applied to generate prediction maps of mercury's spatial distribution, using a base grid cell size of 1 × 1 km for interpolation. To illustrate the spatial patterns of mercury, the correlation among the Hg data was analysed [58]. Spatial autocorrelation means that values at locations close to each other tend to be more similar than those further apart. Once spatial autocorrelation is confirmed, the data can be reliably used for surface estimation methods such as kriging interpolation, which are then used to predict values at unknown points with minimised estimation variance [59,60].

Kriging is a geostatistical approach that estimates a variable's value over a continuous spatial field using a limited number of sampled data points. The variogram $\gamma(h)$ plays a crucial role in universal kriging, quantifying spatial autocorrelation as a function of the lag distance h. It is defined as half the expected squared difference between values separated by distance h:

$$\gamma(h) = \frac{1}{2}E[(Z(\mathrm{s}) - Z(\mathrm{s}+\mathrm{h}))^2]$$

This semi-variogram function is estimated from data and commonly modelled by functions such as spherical, exponential, or linear models to enable interpolation at unsampled locations [32,61–66].

The percentile values of the distribution of all interpolated values (2002/2005/2010/2015) were chosen as class boundaries. Seven classes with the following percentile values were selected: 0–10, 10–25, 25–40, 40–60, 60–75, 75–90, and 90–100. In addition, analysis of variance (ANOVA) revealed significant differences between the four sampling seasons.

3. Results and Discussion

The results of the eighteen-year monitoring of mercury (Hg) contents in mosses in N. Macedonia are summarised in Tables 1 and 2. Table 1 presents the temporal trends of Hg contents in mosses for the sampling years 2002–2020. The data include mean values (X), Box–Cox-transformed mean contents (X_{BC}), median (Md), minimum (Min) and maximum values (Max).

Table 1. Temporal trends of Hg contents in mosses for the sampling years 2002–2020 (in μg/kg).

https://doi.org/10.3390/atmos17010012

Year	X	X_{BC}	Md	Min	Max	P_{25}	P_{75}	S	CV	MAD	QCD	A	E	A_{BC}	E_{BC}
2002	68	58	56	18	264	38	89	40	59	20	40	2.03	7.08	0.01	−0.36
2005	80	60	68	10	416	33	92	72	89	31	48	2.40	7.69	−0.01	0.04
2010	112	91	93	10	595	68	116	94	84	24	26	3.57	14.17	−0.03	4.23
2015	85	79	84	20	253	53	118	47	56	33	39	0.55	0.70	−0.11	−0.49
2020	54	52	52	27	96	43	65	15	28	10	20	0.61	0.14	−0.00	−0.22

X—arithmetic mean, X_{BC}—Box–Cox transformed mean contents; Md—median, Min—minimum, Max—maximum, P_{25}—25 percentiles, P_{75}—75 percentiles, S—standard deviation, CV—coefficient of variation, MAD—mean absolute deviation, QCD—quartile coefficient of dispersion, A—skewness, E—kurtosis, A_{BC}—skewness after Box–Cox transformation, E_{BC}—kurtosis after Box–Cox transformation.

The results indicate significant temporal variability in mercury (Hg) deposition. The highest mean Hg concentration of 112 μg/kg was recorded in 2010, corresponding to the peak background level of 91 μg/kg and an extreme outlier value of 595 μg/kg. In contrast, 2020 exhibited the lowest mean concentration of 54 μg/kg, accompanied by a considerably reduced variability with values ranging from 27 to 96 μg/kg. This observed downward trend between 2010 and 2020 suggests a gradual improvement in atmospheric Hg deposition, likely attributable to stricter environmental regulations, reductions in industrial emissions, and shifts in regional energy production and consumption patterns. This interpretation is further supported by the quartile coefficient of dispersion (QCD), which shows decreased variability among samples in recent years compared to earlier sampling campaigns.

Table 2. Spatial distribution of Hg deposition across the regions and geological formations of N. Macedonia (in μg/kg).

Zone	2002	2005	2010	2015	2020
Regions					
Western regions	66	99	131	79	52
Central regions	85	71	87	87	59
Eastern regions	59	64	105	93	52
Geological formations					
Paleogene–Neogene basins	73	72	93	104	55
West Macedonian zone	69	123	152	79	54
Pelagonian massif	77	60	85	66	51
Vardar zone	56	54	78	88	59
Serbo-Macedonian massif	62	66	126	91	51

Table 2 presents the spatial distribution of mercury (Hg) deposition across the regions and principal geological formations of N. Macedonia. Distinct regional patterns are evident, with the highest concentrations generally recorded in the Western Macedonian zone and the Serbo-Macedonian Massif, particularly in 2010, when values reached 152 μg/kg and 126 μg/kg, respectively. These elevated levels likely reflect the influence of local industrial and mining activities, as well as the enduring legacy of historical metallurgical operations. The Pelagonian Massif and the Vardar zone consistently exhibited relatively moderate Hg levels throughout the studied years, while the eastern regions consistently showed elevated levels during the 2010 and 2015 surveys. By 2020, however, Hg concentrations had decreased across all areas and stabilised at similar values (51–59 μg/kg), indicating a homogenisation of Hg deposition across the country. The observed decrease over time aligns with global trends of reducing mercury emissions due to the implementation of international agreements and stricter environmental regulations. In N.

Macedonia, the closure of obsolete industrial facilities, reduced use of coal in power generation, and improved emission control technologies may have contributed to this decrease. Additionally, the significant decrease in maximum values and overall variability between 2010 and 2020 indicates less influence from sporadic high-emission events or local sources.

Figure 2 shows the Hg contents in moss samples from different regions and tectonic units of N. Macedonia for the period 2002–2020. Compared to previous campaigns, the 2020 dataset confirms a clear downward trend. In 2005, the mean Hg values in the various regions reached approximately 75 μg/kg, decreased to about 65 μg/kg in 2010, and further declined to 55–60 μg/kg by 2015. The 2020 results (45–60 μg/kg), therefore, indicate a continuation of this long-term decline, reflecting the effects of reduced industrial emissions and stricter environmental regulations. In 2020, the values are relatively consistent, ranging between 45 and 60 μg/kg. The highest contents were found in the central regions, followed by the Pelagonian Massif, while the lowest values were observed in the West Macedonian and Vardar zones. This homogenisation contrasts with previous surveys; in 2010, peak values of 152 and 126 μg/kg were measured in the Western Macedonian zone and the Serbo-Macedonian Massif, respectively, indicating the past influence of local industrial and mining activities.

From an environmental health perspective, these results are significant. While previous values exceeded European background levels, the most recent results align more closely with the continental average, suggesting a lower risk of Hg accumulation in soils, vegetation, and the food chain. Nevertheless, the historically elevated contents in industrial areas highlight the need for continuous biological monitoring, given the persistence of mercury, its bioaccumulative potential, and its neurotoxic effects.

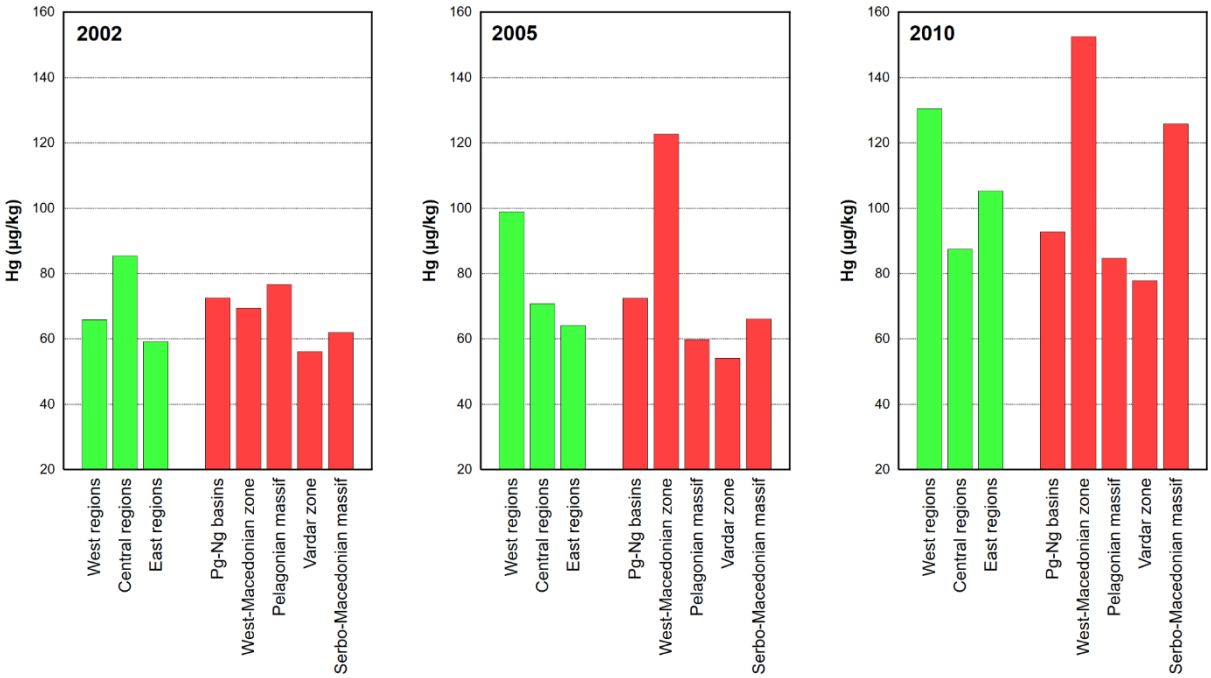

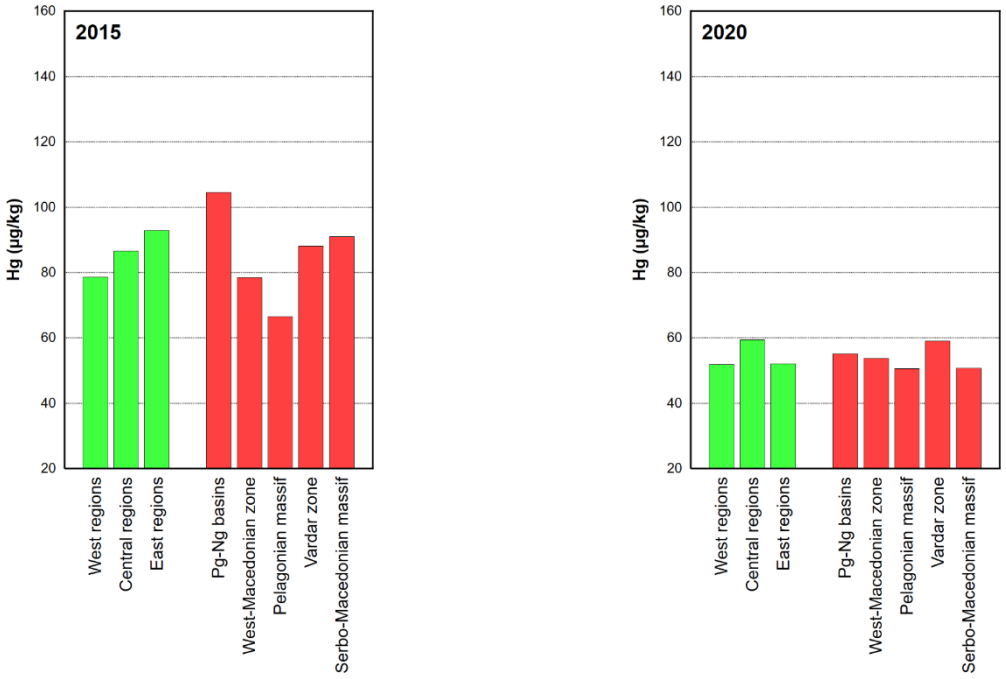

Figure 2. Histograms of the median content of Hg deposition by region and tectonic unit during the study period.

Table 3 summarises the results of the analysis of variance (ANOVA), highlighting the significant key elements that influence mercury (Hg) deposition. The F-value associated with the time variable marked as "year" was highly significant (F = 9.47, $p < 0.01$), confirming strong evidence of marked temporal variation in Hg deposition over the study period. In contrast, regional differences were not statistically significant, suggesting that temporal variation outweighs broad east–west gradients. However, the identified geological formations showed a marginally significant effect (F = 2.61, $p < 0.05$), indicating localised influences from geogenic and industrial sources. These results highlight the importance of long-term monitoring to capture the temporal dynamics of Hg deposition, rather than relying solely on spatial patterns from a single survey.

Table 3. Results of the analysis of variance (ANOVA).

	Degree of Freedom	Sum of Squares	Mean Squares	F Ratio
Year	4	0.13	0.03	9.47 *
Regions	2	0.00	0.00	0.25 ^{NS}
Geoformations	4	0.04	0.01	2.61 *
Error	348	1.23	0.00	–
Total	358	1.41	–	–

* – Statistically significant values ($p = 0.05$); NS – no statistical signification.

Table 4 presents the correlation coefficients between the sampling years, revealing distinct temporal patterns. A moderately strong positive correlation was observed between recent years (2015–2020; r = 0.29), indicating a consistent pattern of mercury deposition during the period of declining Hg emissions. In contrast, earlier years (2002, 2005, 2010) showed weaker or even negative correlations with later surveys, suggesting major changes in emission sources and atmospheric transport mechanisms occurred between 2010 and 2015. These shifts align with the regional declines in Hg emissions reported by the European Environment Agency (EEA) [67] and correspond to wider European trends of declining atmospheric Hg deposition following the introduction of stricter regulatory

emission controls. Such changes in correlation structure reflect the dynamic environmental responses following policy interventions and industrial transformations, highlighting how mercury deposition patterns evolve in response to emission control measures and atmospheric processes

Table 4. Correlation matrix between survey years.

2002	1.00				
2005	−0.01	1.00			
2010	−0.09	−0.00	1.00		
2015	0.06	−0.13	0.08	1.00	
2020	0.04	0.21	0.16	0.29	1.00
	2002	2005	2010	2015	2020

The observed decline in N. Macedonia reflects trends in European moss biomonitoring, where Hg contents have decreased significantly since the early 1990s [68]. Several factors have likely contributed to this: the closure or modernisation of obsolete metallurgical plants, reduced coal consumption, and improved industrial emission controls. At the international level, the Minamata Convention on Mercury, 2023 [69], has further strengthened commitments to reduce Hg releases and established a regulatory framework that also benefits regional air quality.

Figure 3 shows the temporal variation in Hg contents in mosses from N. Macedonia during the five national surveys in 2002, 2005, 2010, 2015 and 2020. The boxplots display medians, interquartile ranges (P_{25}–P_{75}), and whiskers (P_{05}–P_{95}), while the red line highlights the trend of the median values.

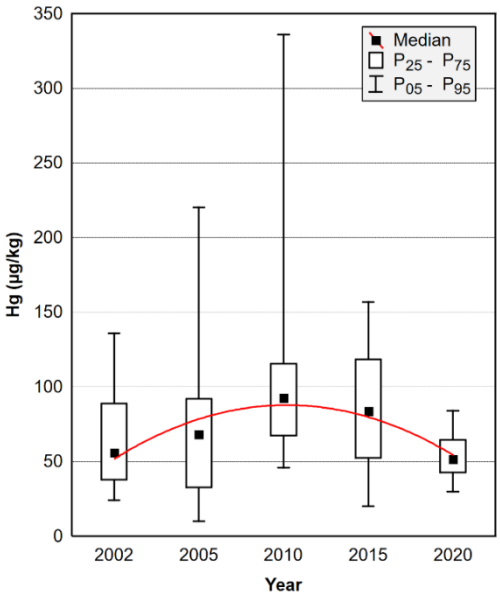

Figure 3. Temporal variation in Hg contents in mosses from N. Macedonia over the five national surveys (2002, 2005, 2010, 2015, 2020).

The distribution clearly illustrates both the temporal dynamics and changes in variability of mercury (Hg) levels. Between 2002 and 2010, the median Hg content increased steadily, reaching a peak of approximately 90 µg/kg in 2010. This period also exhibits the greatest variability, with extreme values exceeding 300 µg/kg, indicating a strong influence from local emission sources and possible episodes of high deposition events. In contrast, the 2015 survey shows a moderate decrease in median values but still a wide interquartile range, indicating transitional conditions. By 2020, Hg levels had decreased

significantly, with the lowest median (~50 μg/kg) and least dispersion of values, showing both a reduction in absolute content and greater uniformity between sampling sites.

The pattern shown in this figure confirms the statistical results presented in Tables 1 and 3, where the "year" factor was found to be highly significant in determining Hg levels. The initial increase up to 2010 probably reflects ongoing industrial and energy-related emissions, while the sharp decline thereafter is consistent with regional and European trends in reducing mercury emissions. Similar trajectories have been documented in moss monitoring in Europe [68], where Hg levels decreased by over 50% between 1990 and 2015.

Importantly, the reduction in variability over time (narrower P_{25}–P_{75} and P_{05}–P_{95} ranges in 2020) suggests that mercury deposition has become more spatially homogenised, reflecting the reduced role of local hotspots with high emissions. This homogenisation is consistent with the decline of large point sources, the modernisation of industrial facilities and the reduced use of coal in N. Macedonia.

The temporal dynamics reveal clear shifts in the "hotspots" of Hg deposition over the eighteen years. In 2002 and 2005, increased contents were observed mainly in the western and southwestern regions, as well as in parts of Central Macedonia. By 2010, the spatial extent of high Hg contamination had expanded considerably, covering large areas in the west, centre, and east of the country. In that year, the highest national average (112 μg/kg) and maximum (>500 μg/kg) levels were recorded, reflecting both regional and long-range transport contributions.

In 2015, the intensity of hotspots remained pronounced, particularly in the east and northeast of the country, although mean values began to decrease compared to 2010. By 2020, the spatial distribution had changed considerably: zones with high contents largely disappeared, and most of the country exhibited moderate to low values (37–74 μg/kg). The homogenisation of contents across the country is consistent with the boxplot results (Figure 1) and supports the statistical evidence (Table 3) that temporal changes are the dominant factor for Hg deposition.

The map of long-term averages highlights the persistent role of certain regions—particularly Western Macedonia and parts of the Serbo-Macedonian Massif—as recurring hotspots during the study period. These areas are influenced by a combination of industrial activities, historical mining and metallurgical operations, and potential geogenic contributions. However, the overall decrease observed in 2020 aligns with international evidence of declining atmospheric Hg following the introduction of stricter emission controls in Europe [68,69].

From an environmental and health perspective, the reduction and spatial minimisation of hotspots is a positive development, as it reduces the potential risk of Hg entering soils, crops, and food chains. Nevertheless, the persistence of historically elevated levels in the long-term average underscores the importance of continuous biomonitoring, especially in regions with an industrial and mining history.

Overall, the eighteen-year assessment demonstrates that moss biomonitoring is an effective tool for tracking temporal trends and spatial patterns of Hg deposition. The results indicate significant improvements in air quality and mercury pollution control in N. Macedonia, while highlighting the need for sustained monitoring to ensure that the observed positive trends are maintained in line with the objectives of the Minamata Convention on Mercury, 2023 [69] (Figure 4).

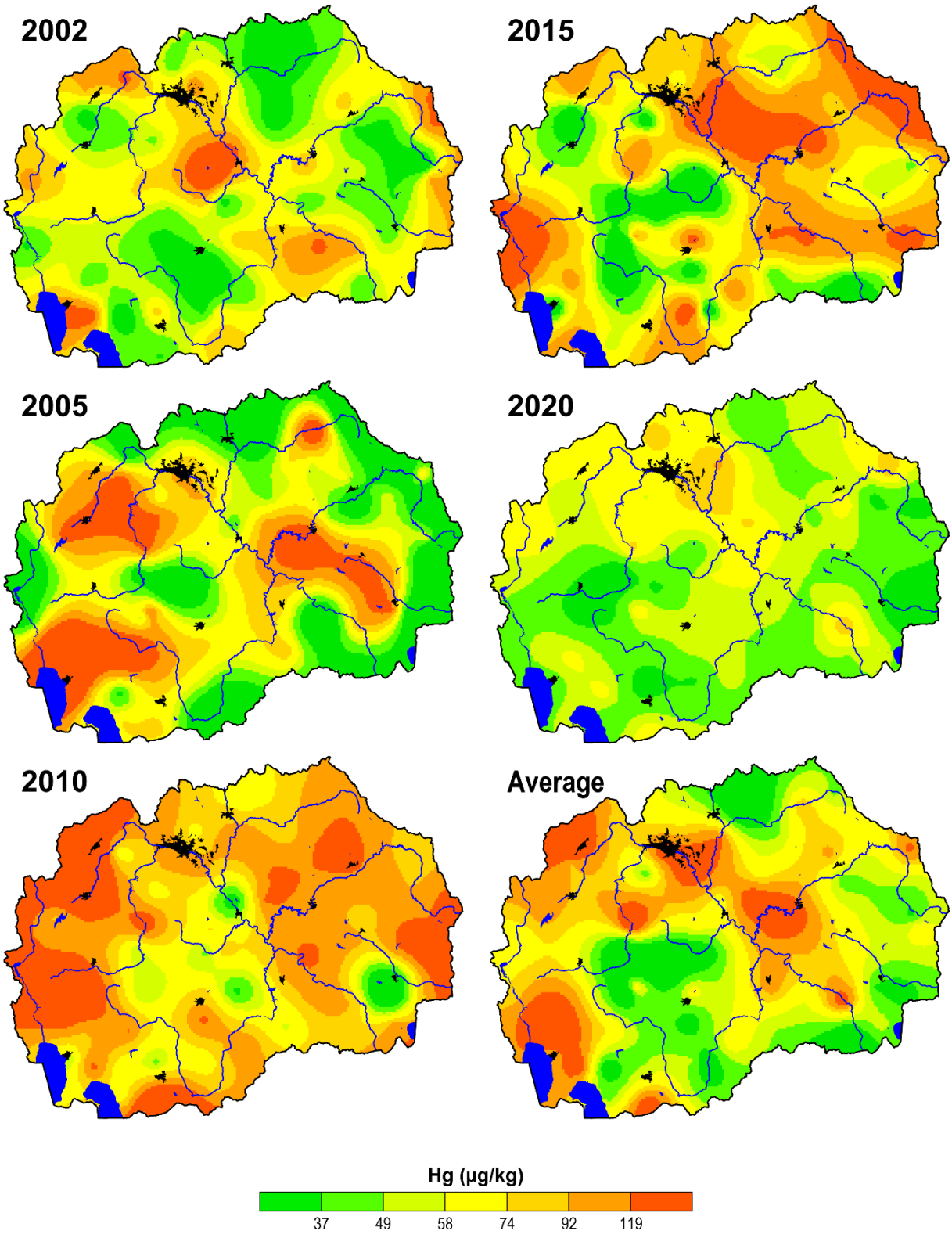

Figure 4. Spatial distribution of Hg contents in mosses in N. Macedonia for the five survey years (2002, 2005, 2010, 2015, and 2020) and the long-term average (2002–2020).

4. Conclusions

This eighteen-year assessment of mercury (Hg) deposition in N. Macedonia, using mosses as bioindicators, provides clear evidence of the temporal and spatial dynamics of atmospheric Hg pollution. The findings demonstrate a marked increase in Hg concentrations until 2010, when both the national mean and extreme values reached their peak,

followed by a consistent decline until 2020. The most recent survey revealed a significant reduction in Hg contents, which were more homogeneously distributed across the country, suggesting reduced influence from localised emission sources with high pollutant levels. The analysis of variance confirmed that temporal fluctuations were the dominant factor for Hg deposition, while large regional differences were not statistically significant. The correlation between recent years (2015–2020) indicates a stabilisation of deposition patterns following major emission reductions. Spatial mapping also revealed that, in the past, elevated contents were associated with the western and northeastern industrial and mining regions, although these hotspots have decreased significantly in the recent survey.

The observed decline in mercury (Hg) content aligns with European and global trends and reflects the effectiveness of stricter emission controls, modernisation of industrial facilities, reduced reliance on coal, and international efforts under the Minamata Convention on Mercury. From an environmental and health perspective, the reduction in Hg levels to near-baseline values by 2020 is encouraging, as it reduces the risk of mercury accumulation in soils, plants, and food chains. However, the persistence of old hotspots in the long-term average emphasises the necessity for continuous monitoring, especially in regions where mining and metallurgy were previously carried out. Overall, this study demonstrates the effectiveness of moss biomonitoring as a reliable tool for tracking atmospheric Hg concentrations over time and spatial scales. The results provide valuable baseline information for policymakers and confirm significant progress in air quality management in N. Macedonia. At the same time, they highlight the importance of long-term environmental monitoring to ensure sustainable protection of ecosystems and human health in a sustainable manner.

Author Contributions: Conceptualisation, L.B., T.S. and K.B.A.; Methodology, L.B., T.S. and K.B.A.; Software, J.A. and R.Š.; Validation, R.Š. and J.A.; Formal analysis, K.B.A. and T.S.; Investigation, L.B., T.S. and K.B.A.; Data curation, T.S. and R.Š.; Writing—original draft, K.B.A., T.S. and J.A.; Writing—review & editing, J.A., T.S. and R.Š.; Visualisation, R.Š.; All authors reviewed the manuscript. R.Š. and J.A. provided supervision and final approval for the manuscript. All authors have read and agreed to the published version of the manuscript.

Funding: This research received no external funding.

Institutional Review Board Statement: Not applicable.

Informed Consent Statement: Not applicable.

Data Availability Statement: The original contributions presented in this study are included in the article. Further inquiries can be directed to the corresponding authors.

Conflicts of Interest: The authors declare no conflict of interest.

References

1. WHO. *Health Effects of Particulate Matter*; UN City: Copenhagen, Denmark, 2025.
2. EPA. Particulate Matter (PM) Pollution. Available online: https://www.epa.gov/pm-pollution (accessed on 16 December 2025).
3. Lelieveld, J.; Evans, J.S.; Fnais, M.; Giannadaki, D.; Pozzer, A. The Contribution of Outdoor Air Pollution Sources to Premature Mortality on a Global Scale. *Nature* **2015**, *525*, 367–371. https://doi.org/10.1038/nature15371.
4. Zauli-Sajani, S.; Thunis, P.; Pisoni, E.; Bessagnet, B.; Monforti-Ferrario, F.; De Meij, A.; Pekar, F.; Vignati, E. Reducing Biomass Burning Is Key to Decrease PM2.5 Exposure in European Cities. *Sci. Rep.* **2024**, *14*, 10210. https://doi.org/10.1038/s41598-024-60946-2.
5. Muntean, M.; Crippa, M.; Guizzardi, D.; Pagani, F.; Becker, W.; Banja, M.; Schaaf, E.; Simonati, A. *EDGAR v8.1 Global Mercury Emissions*; European Commission, Joint Research Centre (JRC): Brussels, Belgium, 2024.
6. EPA. International Actions Reducing Mercury Emissions and Use. Available online: https://www.epa.gov/international-cooperation/international-actions-reducing-mercury-emissions-and-use (accessed on 16 December 2025).

7. UNEP. Global Mercury Assessment 2018. 2019. Available online: https://www.unep.org/resources/publication/global-mercury-assessment-2018 (accessed on 16 December 2025).
8. Brocza, F.M.; Rafaj, P.; Sander, R.; Wagner, F.; Jones, J.M. Global Scenarios of Anthropogenic Mercury Emissions. *Atmos. Chem. Phys.* **2024**, *24*, 7385–7404. https://doi.org/10.5194/acp-24-7385-2024.
9. Geyman, B.M.; Streets, D.G.; Thackray, C.P.; Olson, C.L.; Schaefer, K.; Sunderland, E.M. Projecting Global Mercury Emissions and Deposition Under the Shared Socioeconomic Pathways. *Earth's Future* **2024**, *12*, e2023EF004231. https://doi.org/10.1029/2023EF004231.
10. Pirrone, N.; Costa, P.; Pacyna, J.M.; Ferrara, R. Mercury Emissions to the Atmosphere from Natural and Anthropogenic Sources in the Mediterranean Region. *Atmos. Environ.* **2001**, *35*, 2997–3006. https://doi.org/10.1016/S1352-2310(01)00103-0.
11. UNEP. *Minamata Convention on Mercury: Progress Report 2024*; UNEP: Athens, Greece, 2025.
12. Tchounwou, P.B.; Ayensu, W.K.; Ninashvili, N.; Sutton, D. Review: Environmental Exposure to Mercury and Its Toxicopathologic Implications for Public Health. *Environ. Toxicol.* **2003**, *18*, 149–175. https://doi.org/10.1002/tox.10116.
13. Rühling, Å.; Tyler, G. An Ecological Approach to the Lead Problem. *Bot. Not.* **1968**, *121*, 321–342.
14. Bargagli, R.; Monaci, F.; Borghini, F.; Bravi, F.; Agnorelli, C. Mosses and Lichens as Biomonitors of Trace Metals. A Comparison Study on Hypnum Cupressiforme and Parmelia Caperata in a Former Mining District in Italy. *Environ. Pollut.* **2002**, *116*, 279–287. https://doi.org/10.1016/S0269-7491(01)00125-7.
15. Paoli, L.; Bandoni, E.; Sanità di Toppi, L. Lichens and Mosses as Biomonitors of Indoor Pollution. *Biology* **2023**, *12*, 1248. https://doi.org/10.3390/biology12091248.
16. Rai, P.K. Impacts of Particulate Matter Pollution on Plants: Implications for Environmental Biomonitoring. *Ecotoxicol. Environ. Saf.* **2016**, *129*, 120–136. https://doi.org/10.1016/j.ecoenv.2016.03.012.
17. Jiang, Y.; Fan, M.; Hu, R.; Zhao, J.; Wu, Y. Mosses Are Better than Leaves of Vascular Plants in Monitoring Atmospheric Heavy Metal Pollution in Urban Areas. *Int. J. Environ. Res. Public Health* **2018**, *15*, 1105. https://doi.org/10.3390/ijerph15061105.
18. Mao, H.-T.; Wang, X.-M.; Wu, N.; Chen, L.-X.; Yuan, M.; Hu, J.-C.; Chen, Y.-E. Temporal and Spatial Biomonitoring of Atmospheric Heavy Metal Pollution Using Moss Bags in Xichang. *Ecotoxicol. Environ. Saf.* **2022**, *239*, 113688. https://doi.org/10.1016/j.ecoenv.2022.113688.
19. Lv, D.; Liu, Y.; Ren, L.; Huo, J.; Zhao, J.; Lu, R.; Huang, Y.; Duan, L. Assessment of Atmospheric Heavy Metal Pollution in Qinghai-Tibet Plateau: Using Mosses as Biomonitor. *J. Hazard. Mater.* **2023**, *459*, 132181. https://doi.org/10.1016/j.jhazmat.2023.132181.
20. Giordano, S.; Adamo, P.; Monaci, F.; Pittao, E.; Tretiach, M.; Bargagli, R. Bags with Oven-Dried Moss for the Active Monitoring of Airborne Trace Elements in Urban Areas. *Environ. Pollut.* **2009**, *157*, 2798–2805. https://doi.org/10.1016/j.envpol.2009.04.020.
21. Ares, A.; Aboal, J.R.; Carballeira, A.; Giordano, S.; Adamo, P.; Fernández, J.A. Moss Bag Biomonitoring: A Methodological Review. *Sci. Total Environ.* **2012**, *432*, 143–158. https://doi.org/10.1016/j.scitotenv.2012.05.087.
22. Salo, H.; Paturi, P.; Mäkinen, J. Moss Bag (Sphagnum Papillosum) Magnetic and Elemental Properties for Characterising Seasonal and Spatial Variation in Urban Pollution. *Int. J. Environ. Sci. Technol.* **2016**, *13*, 1515–1524. https://doi.org/10.1007/s13762-016-0998-z.
23. Salo, H.; Mäkinen, J. Comparison of Traditional Moss Bags and Synthetic Fabric Bags in Magnetic Monitoring of Urban Air Pollution. *Ecol. Indic.* **2019**, *104*, 559–566. https://doi.org/10.1016/j.ecolind.2019.05.033.
24. Fačkovcová, Z.; Vannini, A.; Monaci, F.; Grattacaso, M.; Paoli, L.; Loppi, S. Effects of Wood Distillate (Pyroligneous Acid) on Sensitive Bioindicators (Lichen and Moss). *Ecotoxicol. Environ. Saf.* **2020**, *204*, 111117. https://doi.org/10.1016/j.ecoenv.2020.111117.
25. Harmens, H.; Buse, A.; Büker, P.; Norris, D.; Mills, G.; Williams, B.; Reynolds, B.; Ashenden, T.W.; Rühling, Å.; Steinnes, E. Heavy Metal Concentrations in European Mosses: 2000/2001 Survey. *J. Atmos. Chem.* **2004**, *49*, 425–436. https://doi.org/10.1007/s10874-004-1257-0.
26. Harmens, H.; Mills, G.; Hayes, F. *Air Pollution and Vegetation: ICP Vegetation Annual Report 2003/2004*; Martinez-Abaigar, J.D., Aboal, J., Alber, R., Alonso, E.I.G., Akinshina, N., Aleksiayenak, Y., Eds.; ICP Vegetation Coordination Centre: Bangor, UK, 2004.
27. Nickel, S.; Schröder, W.; Schmalfuss, R.; Saathoff, M.; Harmens, H.; Mills, G.; Frontasyeva, M.V.; Barandovski, L.; Blum, O.; Carballeira, A.; et al. Modelling Spatial Patterns of Correlations between Concentrations of Heavy Metals in Mosses and Atmospheric Deposition in 2010 across Europe. *Environ. Sci. Eur.* **2018**, *30*, 53. https://doi.org/10.1186/s12302-018-0183-8.

28. Harmens, H.; Norris, D.A.; Sharps, K.; Mills, G.; Alber, R.; Aleksiayenak, Y.; Blum, O.; Cucu-Man, S.-M.; Dam, M.; De Temmerman, L.; et al. Heavy Metal and Nitrogen Concentrations in Mosses Are Declining across Europe Whilst Some "Hotspots" Remain in 2010. *Environ. Pollut.* **2015**, *200*, 93–104. https://doi.org/10.1016/j.envpol.2015.01.036.
29. Frontasyeva, M.; Harmens, H.; Uzhinsky, A.; Abdusamadzoda, D.; Abdushukurov, D.; Adkinson, K.; Aherne, J.; Alber, Y.; Aleksiayenak, Y.; Allajbeu, S.; et al. *Mosses as Biomonitors of Air Pollution: 2015/2016 Survey on Heavy Metals, Nitrogen and POPs in Europe and Beyond*; Joint Institute for Nuclear Research JINR: Dubna, Russia, 2020; ISBN 978-5-9530-0508-1.
30. Harmens, H.; Norris, D.A.; Koerber, G.R.; Buse, A.; Steinnes, E.; Rühling, Å. Temporal Trends in the Concentration of Arsenic, Chromium, Copper, Iron, Nickel, Vanadium and Zinc in Mosses across Europe between 1990 and 2000. *Atmos. Environ.* **2007**, *41*, 6673–6687. https://doi.org/10.1016/j.atmosenv.2007.03.062.
31. Harmens, H.; Norris, D.A.; Koerber, G.R.; Buse, A.; Steinnes, E.; Rühling, Å. Temporal Trends (1990–2000) in the Concentration of Cadmium, Lead and Mercury in Mosses across Europe. *Environ. Pollut.* **2008**, *151*, 368–376. https://doi.org/10.1016/j.envpol.2007.06.043.
32. Nickel, S.; Schröder, W.; Dreyer, A.; Völksen, B. Mapping Spatial and Temporal Trends of Atmospheric Deposition of Nitrogen at the Landscape Level in Germany 2005, 2015 and 2020 and Their Comparison with Emission Data. *Sci. Total Environ.* **2023**, *891*, 164478. https://doi.org/10.1016/j.scitotenv.2023.164478.
33. Harmens, H.; Norris, D.A.; Steinnes, E.; Kubin, E.; Piispanen, J.; Alber, R.; Aleksiayenak, Y.; Blum, O.; Coşkun, M.; Dam, M.; et al. Mosses as Biomonitors of Atmospheric Heavy Metal Deposition: Spatial Patterns and Temporal Trends in Europe. *Environ. Pollut.* **2010**, *158*, 3144–3156. https://doi.org/10.1016/j.envpol.2010.06.039.
34. Bargagli, R. Moss and Lichen Biomonitoring of Atmospheric Mercury: A Review. *Sci. Total Environ.* **2016**, *572*, 216–231. https://doi.org/10.1016/j.scitotenv.2016.07.202.
35. García-Seoane, R.; Antelo, J.; Fiol, S.; Fernández, J.A.; Aboal, J.R. Unravelling the Metal Uptake Process in Mosses: Comparison of Aquatic and Terrestrial Species as Air Pollution Biomonitors. *Environ. Pollut.* **2023**, *333*, 122069. https://doi.org/10.1016/j.envpol.2023.122069.
36. Di Palma, A.; Capozzi, F.; Spagnuolo, V.; Giordano, S.; Adamo, P. Atmospheric Particulate Matter Intercepted by Moss-Bags: Relations to Moss Trace Element Uptake and Land Use. *Chemosphere* **2017**, *176*, 361–368. https://doi.org/10.1016/j.chemosphere.2017.02.120.
37. Fernández, J.A.; Boquete, M.T.; Carballeira, A.; Aboal, J.R. A Critical Review of Protocols for Moss Biomonitoring of Atmospheric Deposition: Sampling and Sample Preparation. *Sci. Total Environ.* **2015**, *517*, 132–150. https://doi.org/10.1016/j.scitotenv.2015.02.050.
38. Barandovski, L.; Cekova, M.; Frontasyeva, M.V.; Pavlov, S.S.; Stafilov, T.; Steinnes, E.; Urumov, V. Atmospheric Deposition of Trace Element Pollutants in Macedonia Studied by the Moss Biomonitoring Technique. *Environ. Monit. Assess.* **2008**, *138*, 107–118. https://doi.org/10.1007/s10661-007-9747-6.
39. Barandovski, L.; Frontasyeva, M.V.; Stafilov, T.; Šajn, R.; Pavlov, S.; Enimiteva, V. Trends of Atmospheric Deposition of Trace Elements in Macedonia Studied by the Moss Biomonitoring Technique. *J. Environ. Sci. Health Part A* **2012**, *47*, 2000–2015. https://doi.org/10.1080/10934529.2012.695267.
40. Barandovski, L.; Stafilov, T.; Sajn, R.; Frontasyeva, M.; Baceva, K. Air Pollution Study in Macedonia Using a Moss Biomonitoring Technique, ICP-AES and AAS. *Maced. J. Chem. Chem. Eng.* **2013**, *32*, 89–107. https://doi.org/10.20450/mjcce.2013.137.
41. Stafilov, T.; Šajn, R.; Barandovski, L.; Andonovska, K.B.; Malinovska, S. Moss Biomonitoring of Atmospheric Deposition Study of Minor and Trace Elements in Macedonia. *Air Qual. Atmos. Health* **2018**, *11*, 137–152. https://doi.org/10.1007/s11869-017-0529-1.
42. Stafilov, T.; Barandovski, L.; Šajn, R.; Andonovska, K.B. Atmospheric Mercury Deposition in Macedonia from 2002 to 2015 Determined Using the Moss Biomonitoring Technique. *Atmosphere* **2020**, *11*, 1379. https://doi.org/10.3390/atmos11121379.
43. Barandovski, L.; Stafilov, T.; Šajn, R.; Frontasyeva, M.; Andonovska, K.B. Atmospheric Heavy Metal Deposition in North Macedonia from 2002 to 2010 Studied by Moss Biomonitoring Technique. *Atmosphere* **2020**, *11*, 929. https://doi.org/10.3390/atmos11090929.
44. Bačeva Andonovska, K.; Stafilov, T.; Šajn, R.; Jordanoska Shishkoska, B.; Pelivanoska, V.; Barandovski, L. Trends in Atmospheric Nitrogen Deposition in Macedonia Studied by Using the Moss Biomonitoring Technique. *Atmosphere* **2024**, *15*, 1297. https://doi.org/10.3390/atmos15111297.
45. Šajn, R.; Alijagić, J.; Ristović, I. Secondary Deposits as a Potential REEs Source in South-Eastern Europe. *Minerals* **2024**, *14*, 120. https://doi.org/10.3390/min14020120.

46. Dimovska, S.; Stafilov, T.; Šajn, R.; Frontasyeva, M. Distribution of Some Natural and Man-Made Radionuclides in Soil from the City of Veles (Republic of Macedonia) and Its Environs. *Radiat. Prot. Dosim.* **2010**, *138*, 144–157. https://doi.org/10.1093/rpd/ncp238.
47. Stafilov, T.; Šajn, R.; Boev, B.; Cvetković, J.; Mukaetov, D.; Andreevski, M.; Lepitkova, S. Distribution of Some Elements in Surface Soil over the Kavadarci Region, Republic of Macedonia. *Environ. Earth Sci.* **2010**, *61*, 1515–1530. https://doi.org/10.1007/s12665-010-0467-9.
48. Bačeva, K.; Stafilov, T.; Šajn, R.; Tănăselia, C.; Makreski, P. Distribution of Chemical Elements in Soils and Stream Sediments in the Area of Abandoned Sb–As–Tl Allchar Mine, Republic of Macedonia. *Environ. Res.* **2014**, *133*, 77–89. https://doi.org/10.1016/j.envres.2014.03.045.
49. Lazarevski, A. *Climate in Macedonia*; Kultura: Skopje, Republic of Macedonia, 1993.
50. Stafilov, T.; Šajn, R. *Geochemical Atlas of the Republic of Macedonia*; Faculty of Natural Sciences and Mathematics, Ss Cyril and Methodius University, Skopje, Republic of Macedonia: Skopje, Republic of Macedonia, 2016; ISBN 978-608-4762-04-1.
51. Steinnes, E.; Rühling, Å.; Lippo, H.; Mäkinen, A. Reference Materials for Large-Scale Metal Deposition Surveys. *Accredit. Qual. Assur.* **1997**, *2*, 243–249. https://doi.org/10.1007/s007690050141.
52. Harmens, H.; Mills, G.; Hayes, F. *Air Pollution and Vegetation: ICP Vegetation Annual Report 2004/2005*; Martinez-Abaigar, J.D., Aboal, J., Alber, R., Alonso, E.I.G., Akinshina, N., Aleksiayenak, Y., Eds.; ICP Vegetation Coordination Centre: Bangor, UK, 2005.
53. Harmens, H.; Mills, G.; Hayes, F. *Air Pollution and Vegetation: ICP Vegetation Annual Report 2011/2012*; Martinez-Abaigar, J.D., Aboal, J., Alber, R., Alonso, E.I.G., Akinshina, N., Aleksiayenak, Y., Eds.; ICP Vegetation Coordination Centre: Bangor, UK, 2012.
54. Snedecor, G.W.; Cochran, W.G. *Statistical Methods*, 6th ed.; The Iowa State University Press: Ames, IA, USA, 1967.
55. Davis, J.C. *Statistics and Data Analysis in Geology*, 3rd ed.; Wiley: Hoboken, NJ, USA, 2002.
56. Hollander, M.; A. Wolfe, D.; Chicken, E. *Nonparametric Statistical Methods*; Wiley: Hoboken, NJ, USA, 2015; ISBN 9780470387375.
57. *Statistica (Software)*, Version 14; TIBCO Software Inc.: Palo Alto, CA, USA, 2020.
58. Matheron, G. Présentation Des Variables Régionalisées. *J. La Société Stat. Paris* **1966**, *107*, 263–275.
59. Krige, D.G. A Statistical Approaches to Some Basic Mine Valuation Problems on the Witwatersrand. *J. Chem. Metall. Min. Soc. S. Afr.* **1951**, *52*, 119–139.
60. Krige, D.G. On the Departure of Ore Value Distributions from Lognormal Models in South African Gold Mines. *J. S. Afr. Inst. Min. Metall.* **1960**, *60*, 231–244.
61. Zhu, Q.; Lin, H.S. Comparing Ordinary Kriging and Regression Kriging for Soil Properties in Contrasting Landscapes. *Pedosphere* **2010**, *20*, 594–606. https://doi.org/10.1016/S1002-0160(10)60049-5.
62. Hu, X.; Zhang, Y.; Luo, J.; Wang, T.; Lian, H.; Ding, Z. Bioaccessibility and Health Risk of Arsenic, Mercury and Other Metals in Urban Street Dusts from a Mega-City, Nanjing, China. *Environ. Pollut.* **2011**, *159*, 1215–1221. https://doi.org/10.1016/j.envpol.2011.01.037.
63. Oliver, M.A.; Webster, R. A Tutorial Guide to Geostatistics: Computing and Modelling Variograms and Kriging. *Catena* **2014**, *113*, 56–69. https://doi.org/10.1016/j.catena.2013.09.006.
64. Ha, H.; Olson, J.R.; Bian, L.; Rogerson, P.A. Analysis of Heavy Metal Sources in Soil Using Kriging Interpolation on Principal Components. *Environ. Sci. Technol.* **2014**, *48*, 4999–5007. https://doi.org/10.1021/es405083f.
65. Liu, G.; Zhou, X.; Li, Q.; Shi, Y.; Guo, G.; Zhao, L.; Wang, J.; Su, Y.; Zhang, C. Spatial Distribution Prediction of Soil As in a Large-Scale Arsenic Slag Contaminated Site Based on an Integrated Model and Multi-Source Environmental Data. *Environ. Pollut.* **2020**, *267*, 115631. https://doi.org/10.1016/j.envpol.2020.115631.
66. Jang, D.; Kim, N.; Choo, H. Kriging Interpolation for Constructing Database of the Atmospheric Refractivity in Korea. *Remote. Sens.* **2024**, *16*, 2379. https://doi.org/10.3390/rs16132379.
67. EEA. Heavy Metal Emission in Europe. Available online: https://www.eea.europa.eu/en/analysis/indicators/heavy-metal-emissions-in-europe (accessed on 16 December 2025).

68. Hayes, F., Sharps, K.; Participants of the Moss Survey. *Mosses as Biomonitors of Air Pollution: 2020/2021 Survey on Heavy Metals, Nitrogen and POPs in Europe and Beyond*; Hayes, F., Sharps, K., Eds.; ICP Vegetation Coordination Centre, UK Centre for Ecology & Hydrology, Environment Centre: Bangor, Wales, UK, 2024.
69. UNEP. *Decisions Adopted by the Conference of the Parties to the Minamata Convention on Mercury at Its Fifth Meeting*; UNEP: Athens, Greece, 2023.